

Supplementary Information

Transformation of nanoparticles via transition of functional DNAs responsive to pH and vascular endothelial growth factor for photothermal anti-tumor therapy

Jinseong Kim^a, Yunyoung Nah^a, Seongmin Kim^a, Won Jong Kim^{a, b, c}*

*^a Department of Chemistry, POSTECH-CATHOLIC Biomedical Engineering Institute,
Pohang University of Science and Technology (POSTECH), Pohang 37673, Republic of
Korea*

*^b School of Interdisciplinary Bioscience and Bioengineering, Pohang University of Science
and Technology (POSTECH), Pohang 37673, Republic of Korea*

^c OmniaMed Co., Ltd., Pohang, Republic of Korea

*e-mail: wjkim@postech.ac.kr

Table S1. DNA sequence used in the experiment. Blue letters indicate the complementary sequence and red letters indicate the split VEGF aptamer fragment.

Sequence name	Sequence
Aptamer fragment A	5'-Thiol-TTTTTTTTTTTGACTGACTATGTCCCGTCTTC-3'
Aptamer fragment B	5'-CAGACAAGAGTGCAGGGGGACATAGTCAGTCATTTTTTTTTT-Thiol-3'
Control fragment A	5'-Thiol-TTTTTTTTTTTGACTGACTATGTCCCTGACTTGG-3'
Control fragment B	5'-TGCATACGATGGCAGGGGGACATAGTCAGTCATTTTTTTTTT-Thiol-3'
i-motif	5'-Thiol-TTTTCCCCTTCCCCTTCCCCTTCCCC-3'
i-motif control	5'-Thiol-TTTTCCAATTGGACTTCCCCTTCAAA-3'
i-motif complimentary	5'-TTTGAAGGGGAAGTCCAATTGG-3'

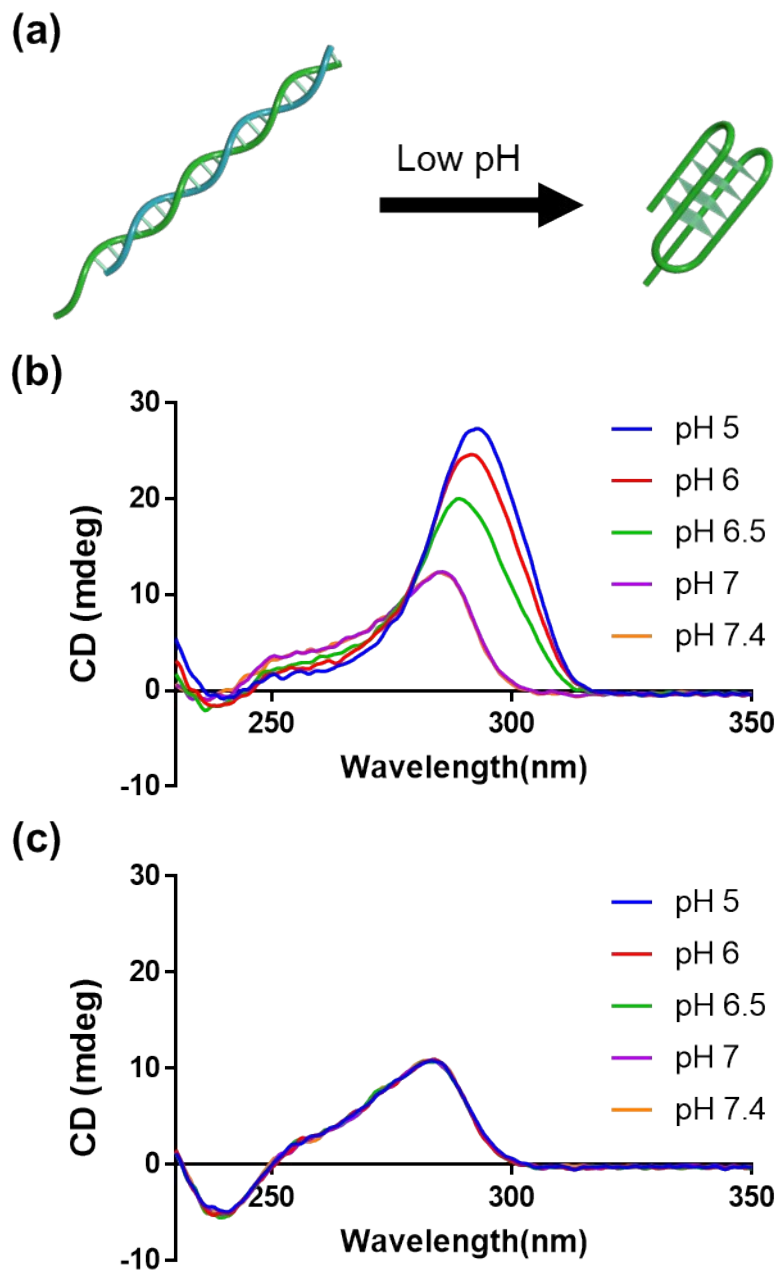


Figure S1. Circular dichroism spectra of i-motif duplex at different pH. (a) Schematic illustration of i-motif duplex transition in response to low pH. (b) i-motif duplex consisting of i-motif and i-motif complementary sequence. (c) i-ctrl duplex consisting of pH-insensitive i-motif control and i-motif complementary sequence.

Table S2. DNAs used in Au-DNAs. Aptamer indicates VEGF aptamer fragment. Aptamer fragment that cannot capture VEGF was used as a Control. i-motif duplex is DNA duplex consisting of i-motif and i-motif complementary sequence. I-ctrl duplex indicates DNA duplex consisting of pH-insensitive i-motif control and i-motif complementary sequence.

	Au-A-IC	Au-B-IC	Au-CA-I	Au-CB-I	Au-A-I	Au-B-I
Aptamer fragment	Aptamer		Control		Aptamer	
DNA duplex	i-motif control		i-motif		i-motif	

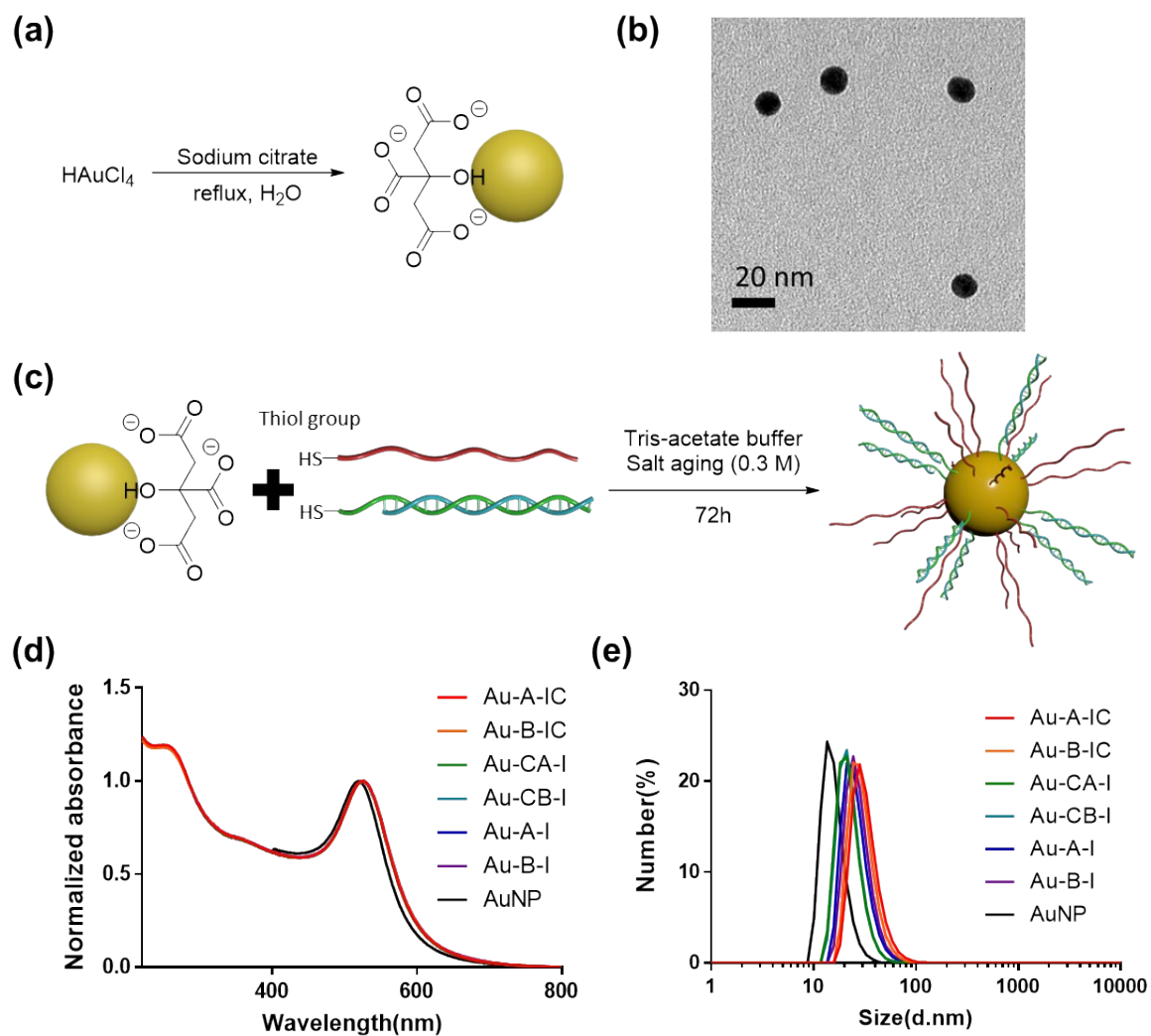


Figure S2. Characterization of AuNP and Au-DNAs. (a) Synthetic method for AuNP. (b) TEM image of AuNP. (c) Synthetic method for Au-DNAs. (d) Absorption spectra of AuNP and Au-DNAs. (e) Hydrodynamic size of AuNP and Au-DNAs.

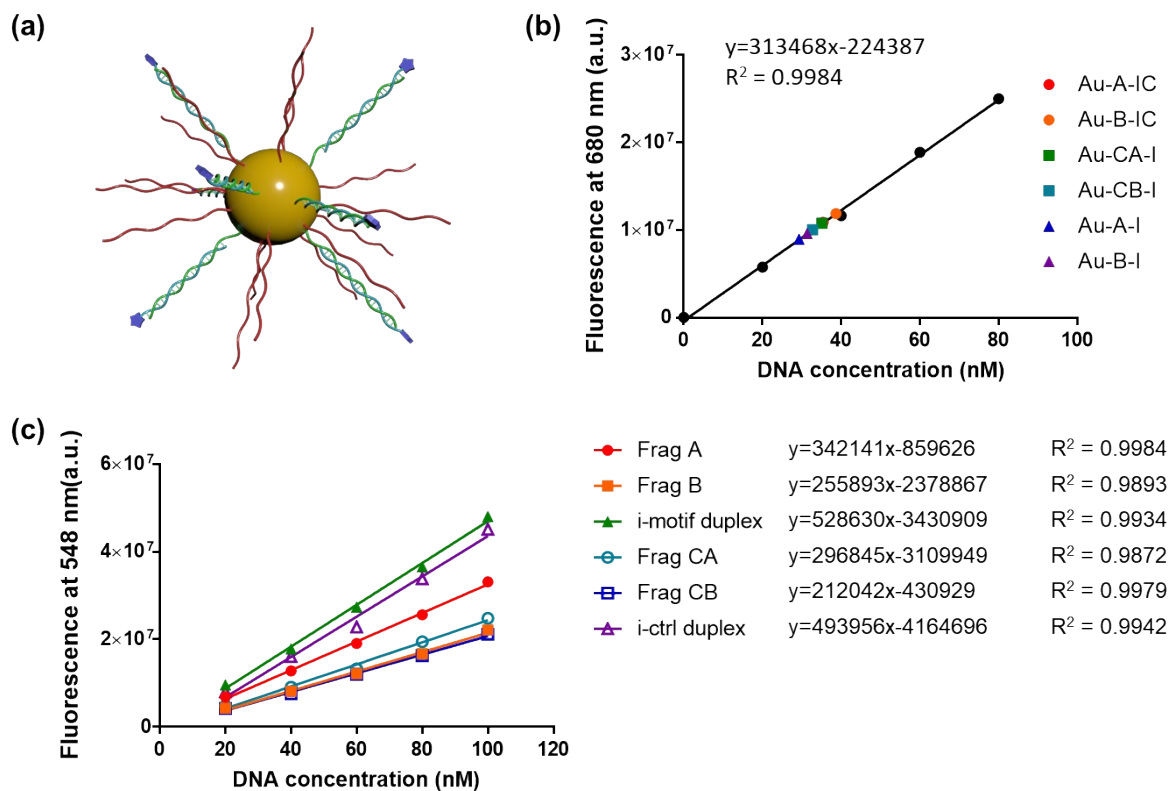


Figure S3. DNA quantification of Au-DNAs. (a) Schematic illustration of Au-DNAs with Cy5-modified i-motif complementary sequence. (b) DNA quantification of i-motif complementary by fluorescence of Cy5. (c) DNA quantification of various sequences by fluorescence of SYBR gold.

Table S3. The amount of DNAs conjugated to each Au-DNAs from figure S3.

	Aptamer fragment	I-motif duplex
Au-A-I	61.8±3.0	29.3±1.2
Au-B-I	55.1±4.0	31.4±2.9
Au-CA-I	62.2±1.6	35.2±0.6
Au-CB-I	56.5±3.0	32.7±1.4
Au-A-IC	64.4±2.7	35.4±2.9
Au-B-IC	55.3±1.6	38.7±1.7

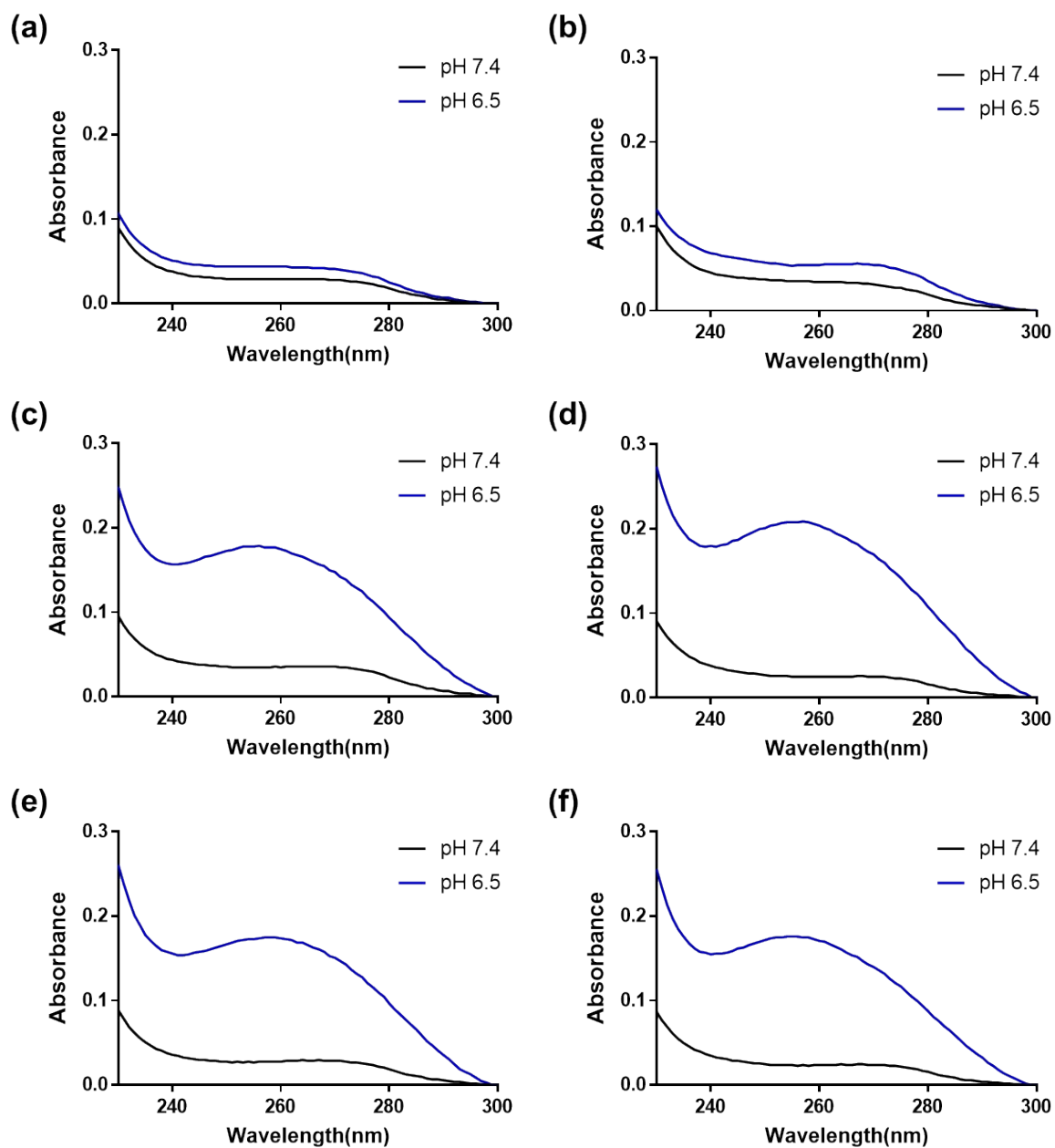


Figure S4. Absorbance spectra of DNA from Au-DNAs at different pH. (a) Au-A-IC, (b) Au-B-IC, (c) Au-CA-I, (d) Au-CB-I, (e) Au-A-I and (f) Au-B-I.

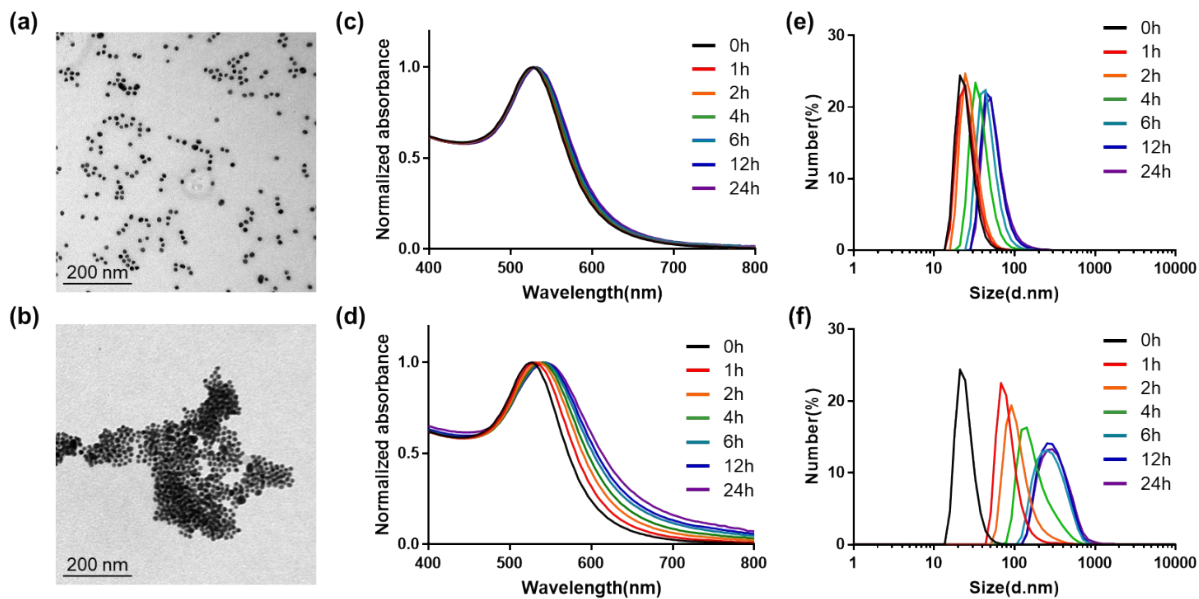


Figure S5. pH-responsive behavior of Au-CA-I + Au-CB-I. (a-b) TEM image of Au-CA-I + Au-CB-I after 24 h incubation, (a) at pH 7.4, (b) at pH 6.5. (c-d) Absorbance spectra of Au-CA-I + Au-CB-I for different time interval, (c) at pH 7.4, (d) at pH 6.5. (e-f) hydrodynamic size of Au-CA-I + Au-CB-I for different time interval, (e) at pH 7.4, (f) at pH 6.5.

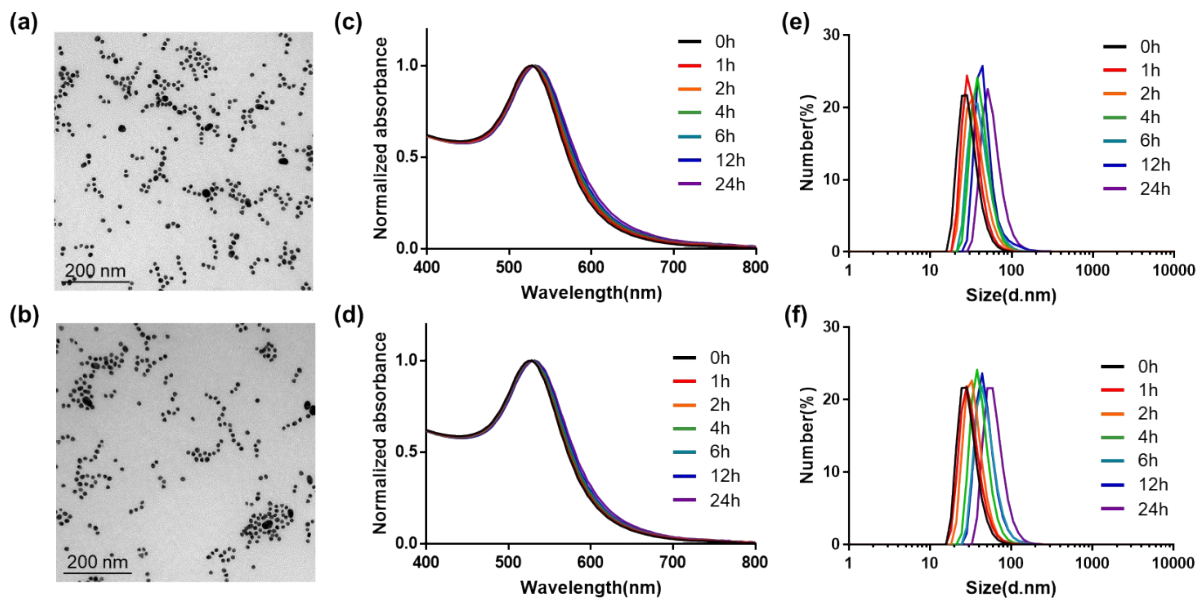


Figure S6. pH-responsive behavior of pH-non-responsive Au-A-IC + Au-B-IC. (a-b) TEM image of Au-A-IC + Au-B-IC after 24 h incubation, (a) at pH 7.4, (b) at pH 6.5. (c-d) Absorbance spectra of Au-CA-I + Au-CB-I for different time interval, (c) at pH 7.4, (d) at pH 6.5. (e-f) hydrodynamic size of Au-A-IC + Au-B-IC for different time interval, (e) at pH 7.4, (f) at pH 6.5.

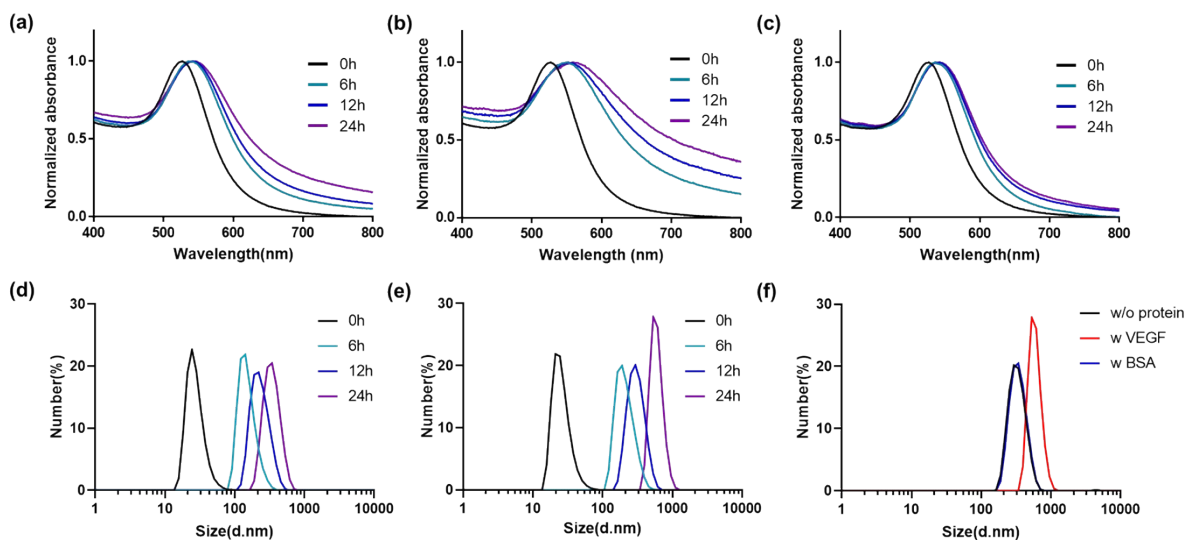


Figure S7. Protein-responsive aggregation of Au-DNAs at pH 6.5. (a-c) Absorbance spectra of (a) Au-A-I + Au-B-I w BSA, (b) Au-A-I + Au-B-I w VEGF and (c) Au-CA-I + Au-CB-I w VEGF for different time interval. (d-e) hydrodynamic size of (d) Au-A-I + Au-B-I w BSA and (e) Au-A-I + Au-B-I w VEGF. (f) Hydrodynamic size of Au-A-I + Au-B-I with or without protein after 24 h incubation.

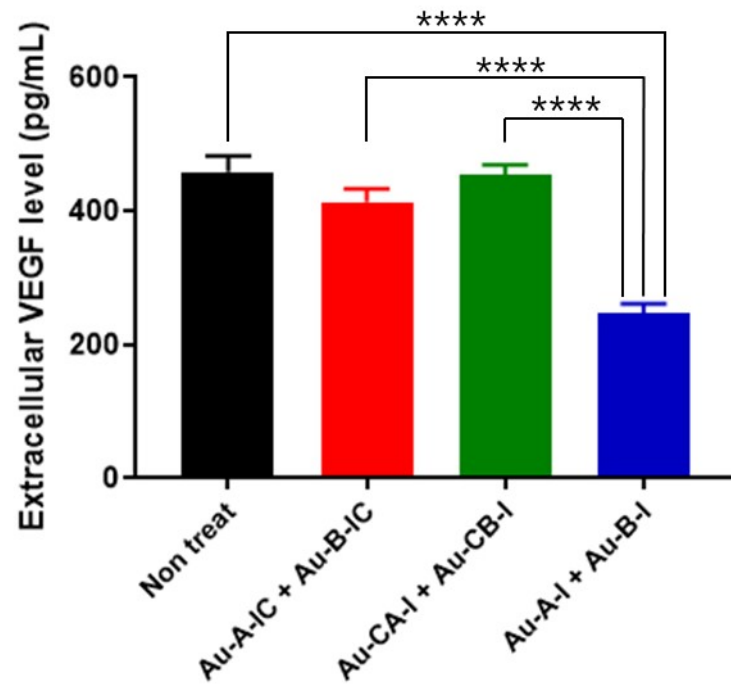


Figure S8. *In vitro* extracellular VEGF level. Data represent the mean \pm SD (n=5, **** p < 0.0001).

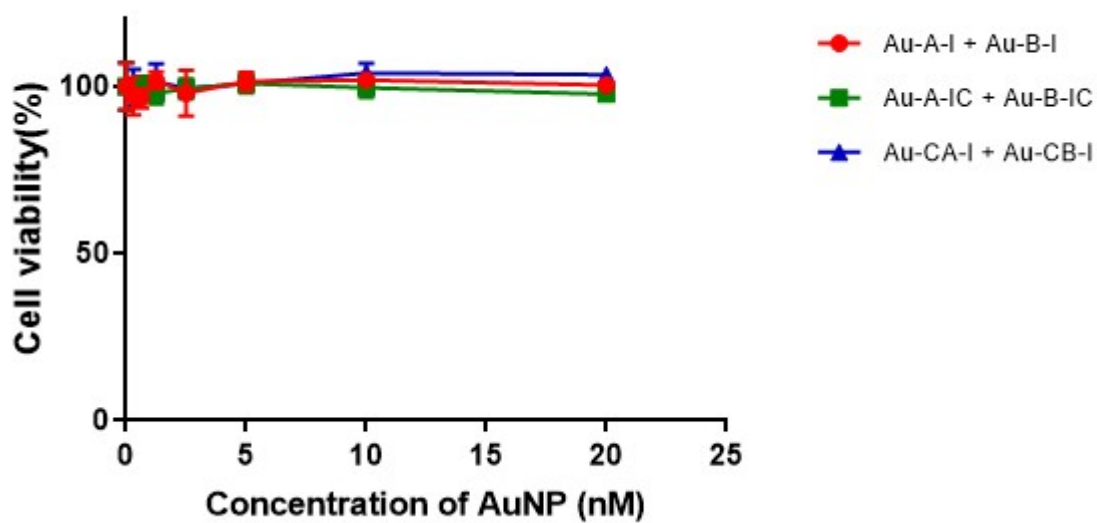


Figure S9. Cell viability of MCF-7 treated with various concentration of Au-DNAs (n=5).

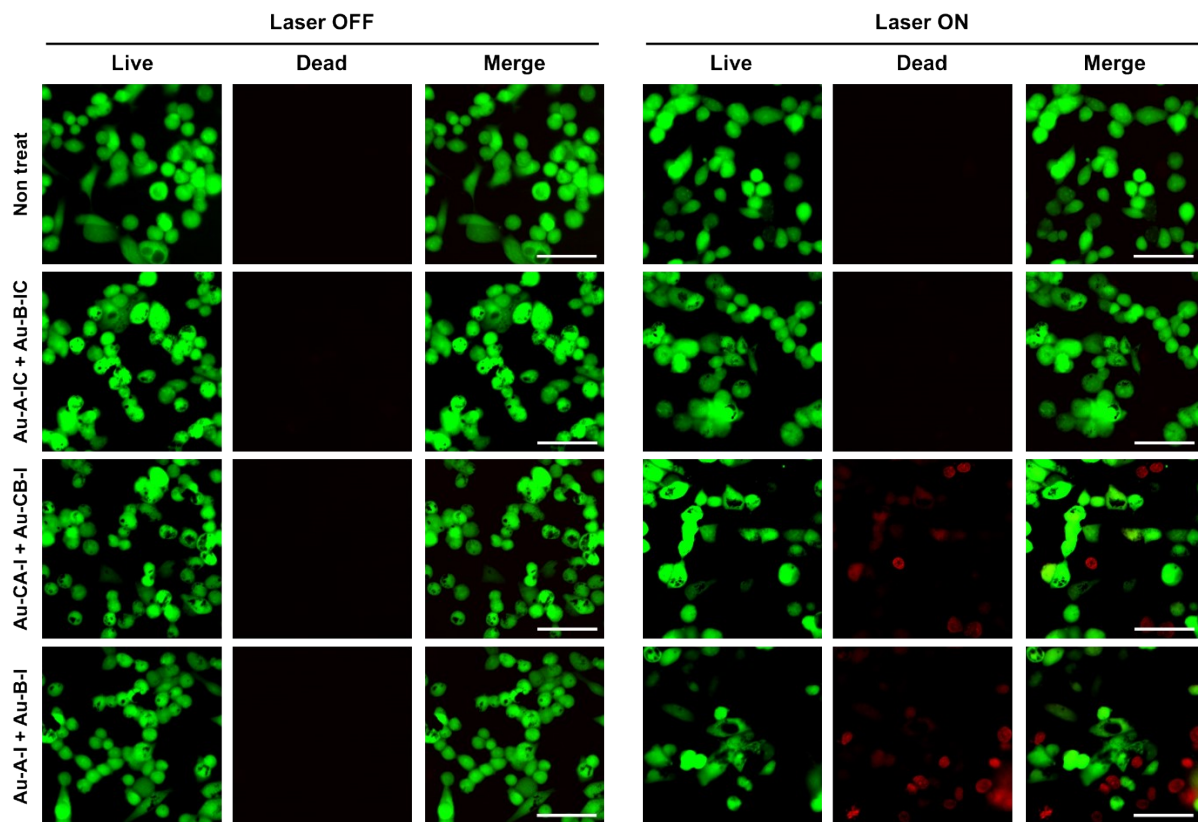


Figure S10. Fluorescent image of MCF-7 cells treated with Au-DNAs, with and without 808 nm laser irradiation (3 W cm^{-2}) (Scale bar = $50 \mu\text{m}$).

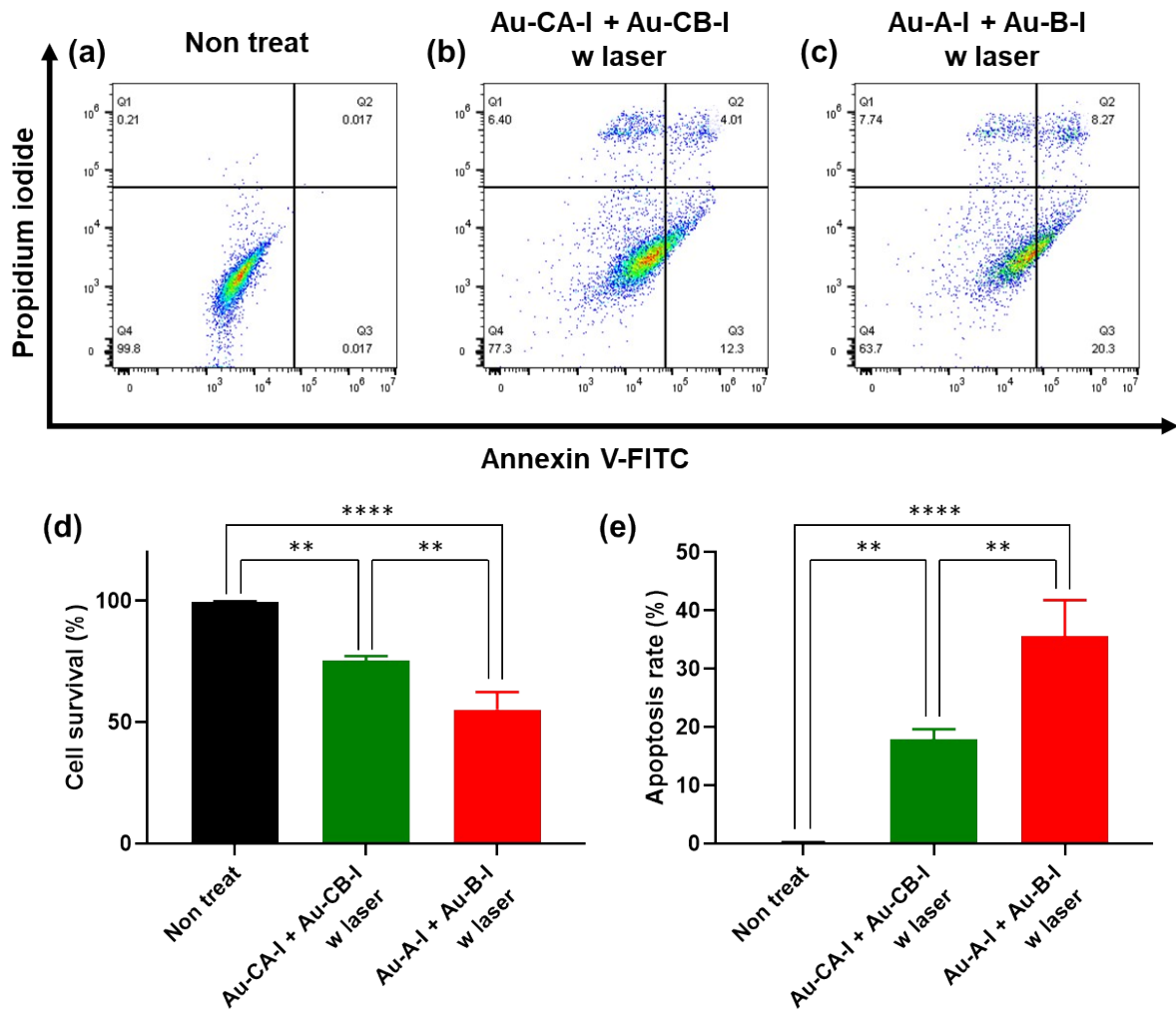


Figure S11. Apoptosis of MCF-7 cells induced by Au-DNAs mediated PTT. (a-c) Representative plots of annexin V-FITC/PI-stained cells treated with (a) non treat, (b) Au-CA-I + Au-CB-I with laser irradiation and (c) Au-A-I + Au-B-I with laser irradiation. (d) Rate of survival cells. (e) Rate of apoptosis cells. Data represent the mean \pm SD ($n=3$, ** $p < 0.01$, **** $p < 0.0001$).

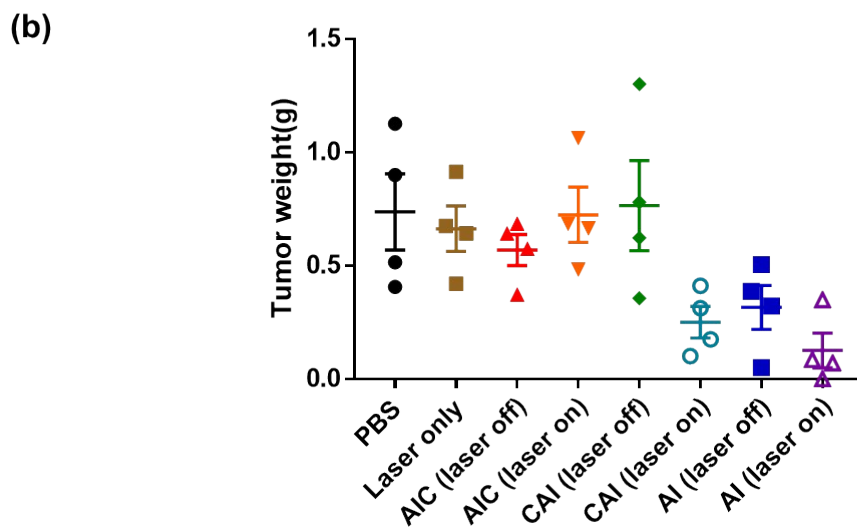
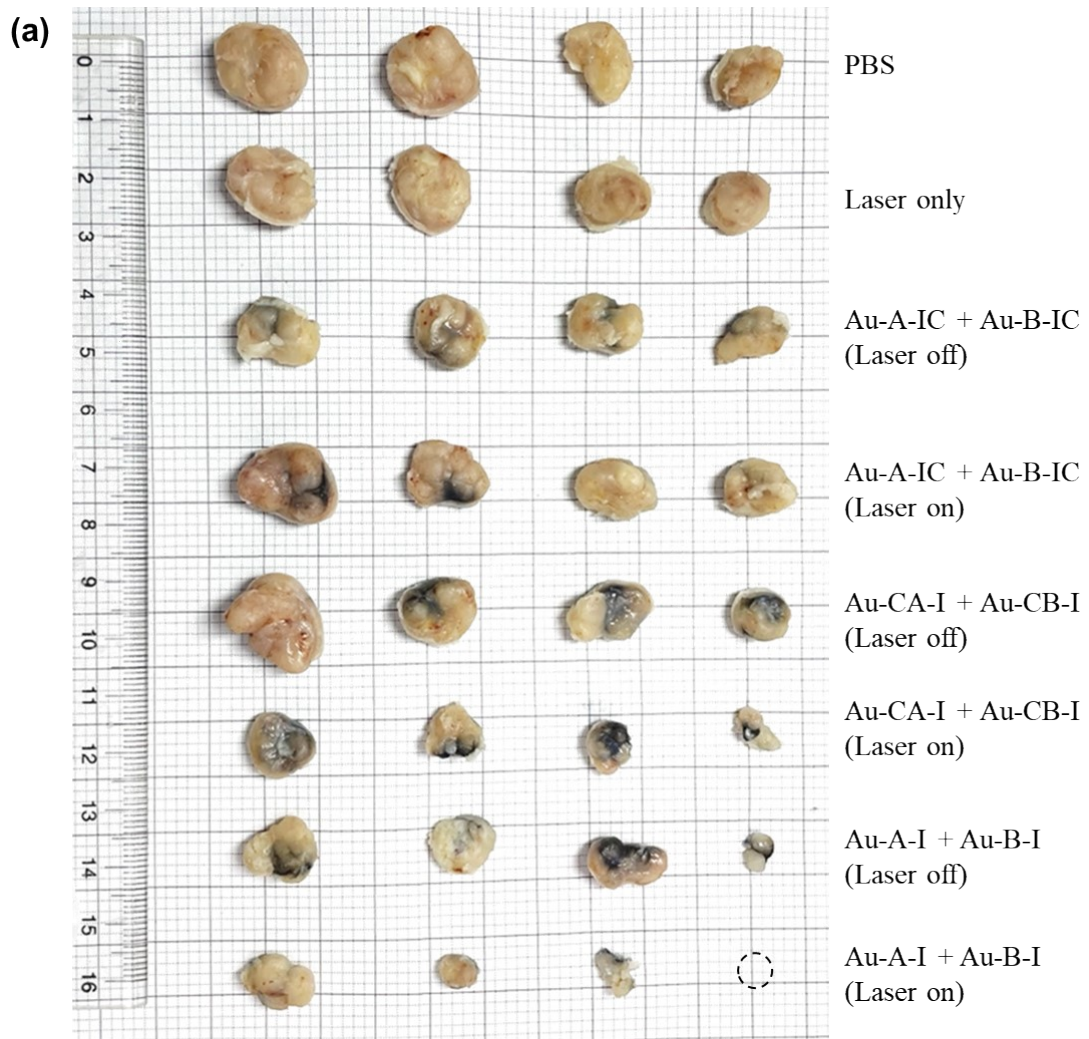


Figure S12. Surgically removed tumor tissues from mice on day 22. (a) Image of tumor. (b) Tumor weight.